FIGURES

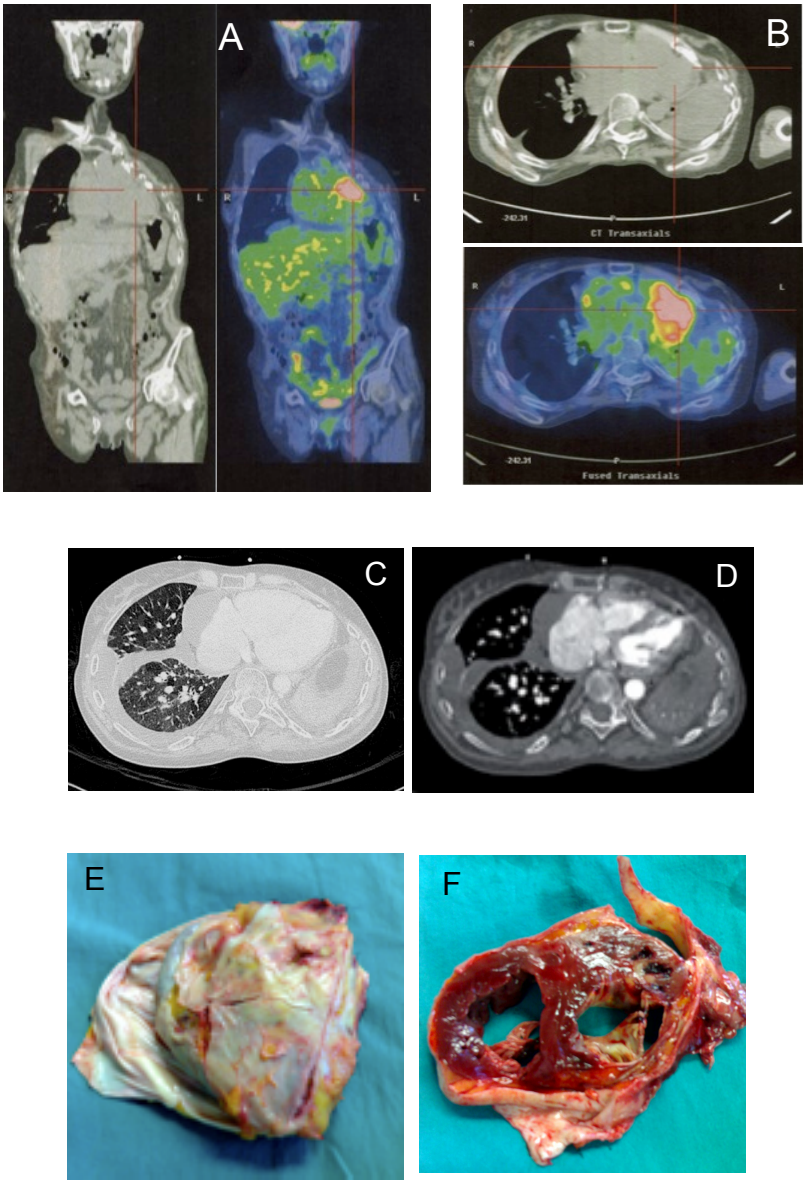

Figure 1. Longitudinal total body (A) and thoracic transaxial (B) views of PET scan and CAT scan of thoracic parenchymal window (C and D) taken 31 years after therapy. Collapse of the left lung, dislocation of mediastinal organs, and pleural and pericardial effusions are present. The right lung also shows scissural thickening (C). E: autoptic heart with pericardial thickening. F: transverse section of the heart at autopsy documenting extensive left ventricular damage and calcific percarditis.

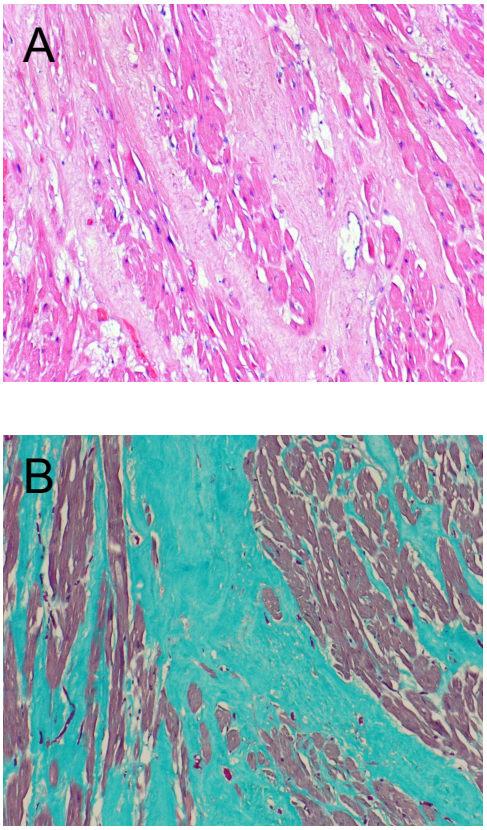

Figure 2. Light microscopy of Hematoxilin & Eosin (A) stained section of the heart obtained at autopsy from the patients of Autoptic Case 1, documenting foci of acute damage and extensive myocardial fibrosis best seen in Trichrome Masson's (B) staining of the serial section.

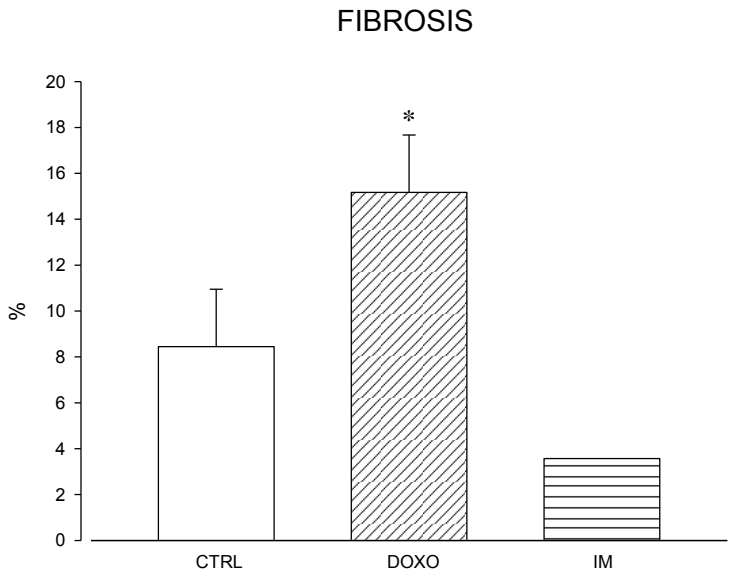

Figure 3. Volumetric fraction of fibrosis in hearts of patients treated with DOXO and in the heart of the patient treated with IM.

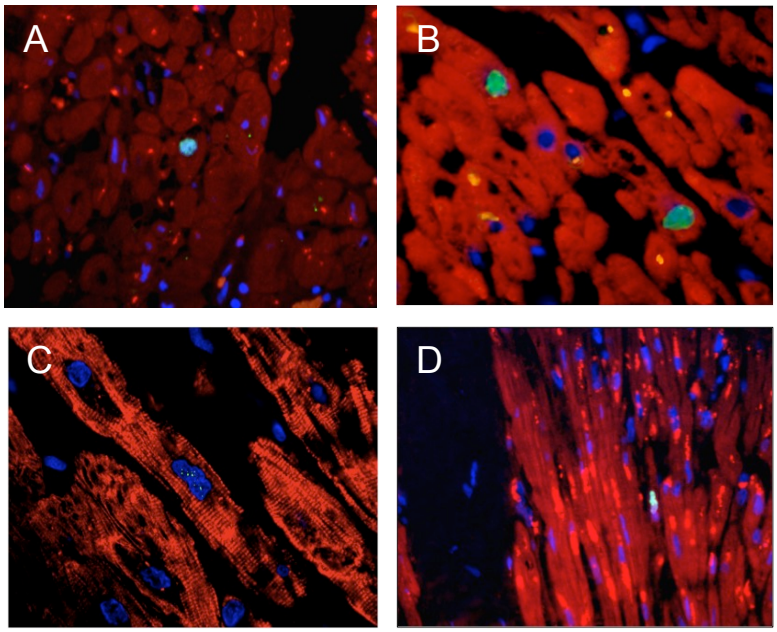

Figure 4. Immunofluorescence images of sections of the human left ventricular myocardium from a Doxo-induced cardiomyopathy. Green fluorescence indicates the nuclear expression of gH2AX (A), for the detection of DNA double strand breaks, and apoptosis (B) by Tunel in cardiomyocytes. In C and D green fluorescence indicate respectively cycling cardiomyocytes as detected by the nuclear expression of the antibody against minichromosome maintenance protein 5 (MCM5) and nuclear expression of the phophorylated form of Histone H3, Cardiomyocytes are recognized by the red fluorescence of α-sarcomeric actin antibody and nuclei by the blue fluorescence of DAPI.

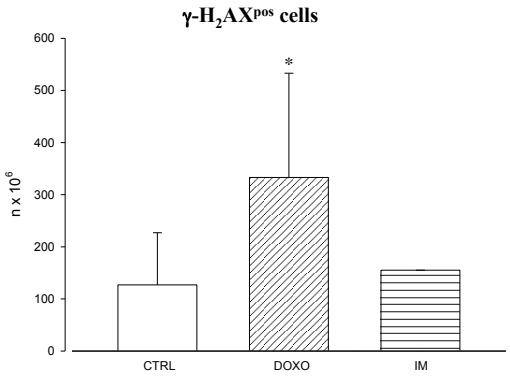

Figure 5. Bar graphs documenting DNAdSB in cardiomyocytes evaluated by nuclear expression of γ-H_2AX, in patients treated with DOXO and in the single patient treated with IM. CTRL: control; *p<0.05 vs CTRL.

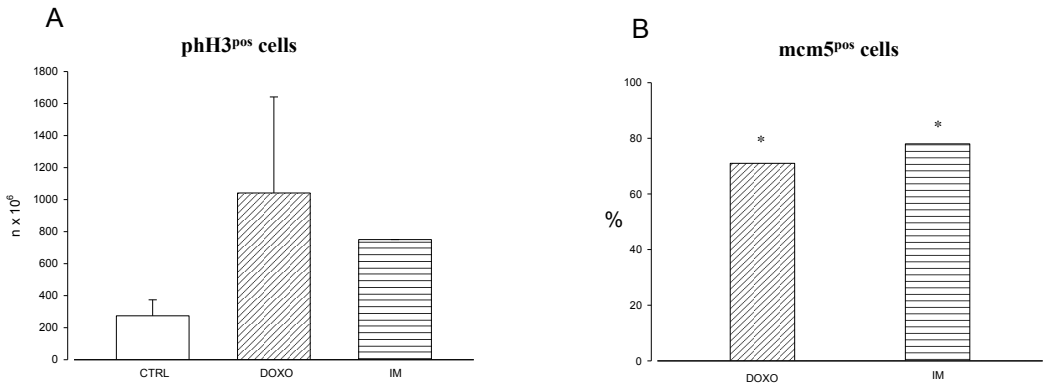

Figure 6. Graph A document mitotic division (A) in cardiomyocytes detected by nuclear expression of pH-H3 in DOXO and IM treated hearts.; *p<0.05 vs CTRL. Graph B show the difference in percentage of mcm5 pos cells (cycling cells) in patients treated with chemotherapic drugs respect ctrl heart. CTRL: control

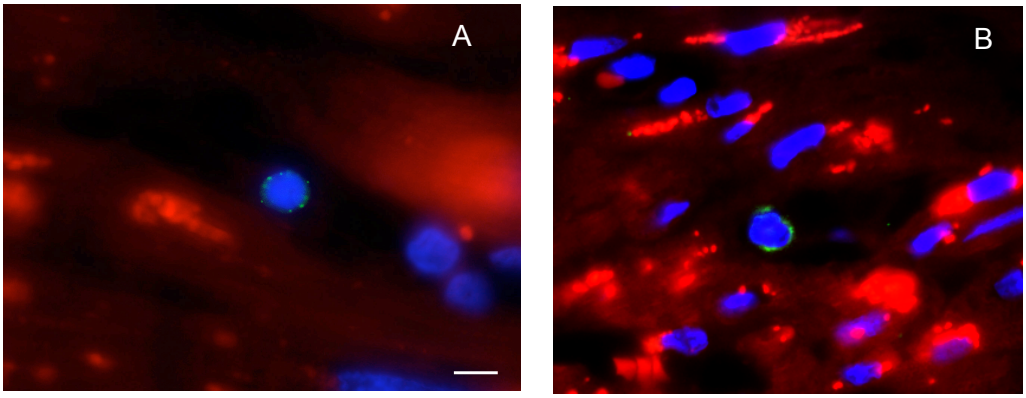

Figure 7. Immunohistochemical detection of the surface expression of c-kit (green fluorescence) in an interstitial cell in close contact with α-sarcomeric actin positive cardiomyocytes (red fluorescence) in the patient died during IM treatment (A) and in a patient treated with DOXO (B). Blue fluorescence corresponds to DAPI staining of nuclei. Scale Bar=10 μm.

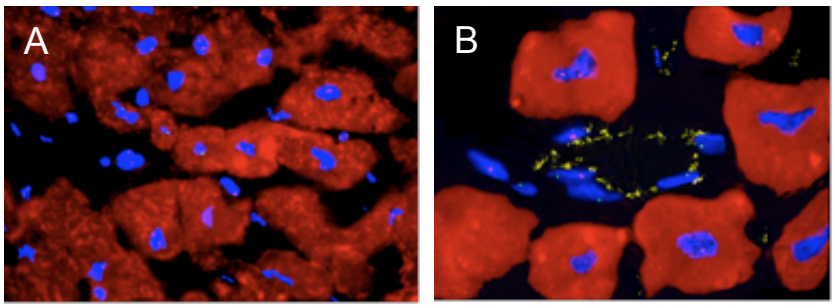

Figure 8. Cardiac Chimerism. Cardiomyocytes (A) and vascular structures (B) showing Y chromosome (green fluorescent dots) present in the autoptic case 1, 25 years after delivery of a healthy boy. Cardiomyocytes are recognized by the red fluorescence of α-sarcomeric actin antibody. B: yellow fluorescence corresponds to von Wilebrand Factor. Chromosome X and Y, as detected by FISH analysis, correspond to red and green fluorescent dots, respectively. Blue fulorescence corresponds to DAPI staining of nuclei.

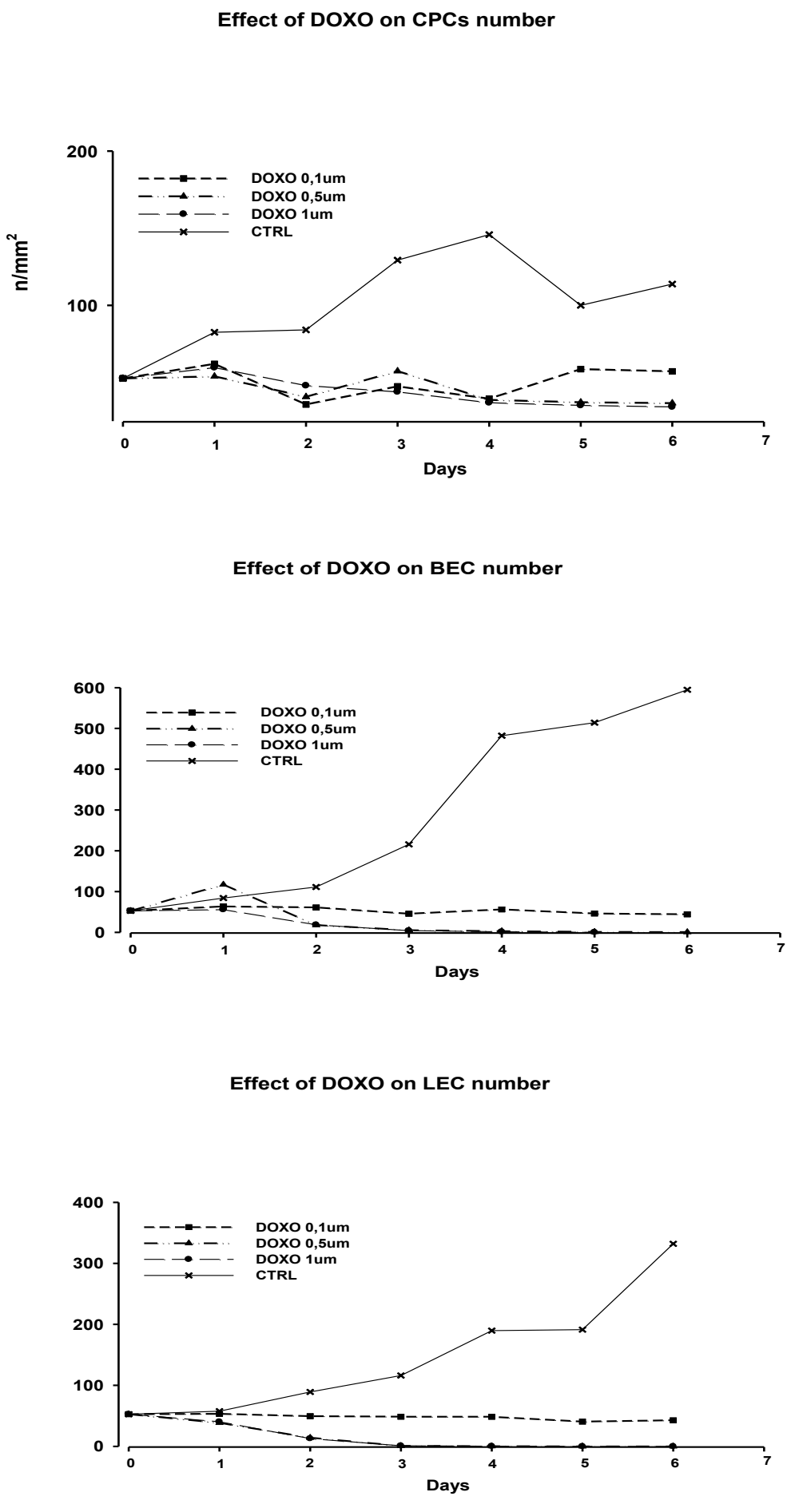

Figure 9. Effects of in vitro treatment with DOXO on hCPC, hBEC and hLEC.

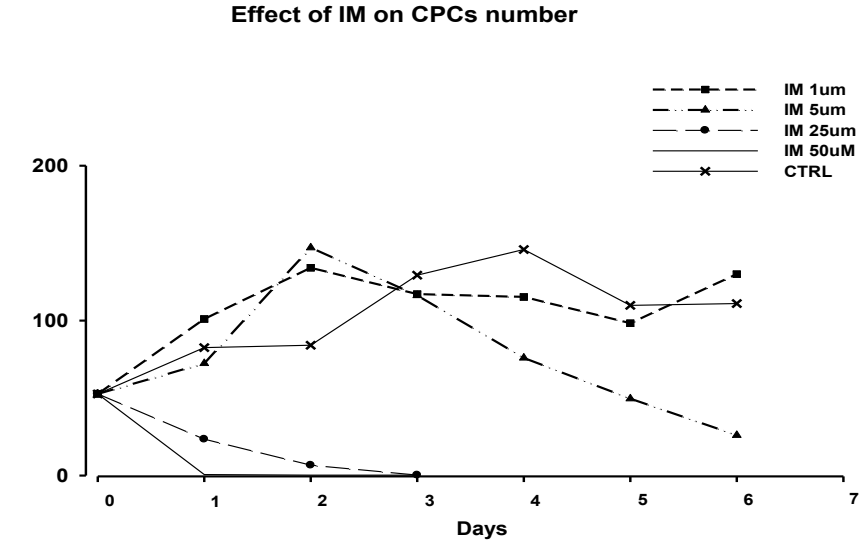

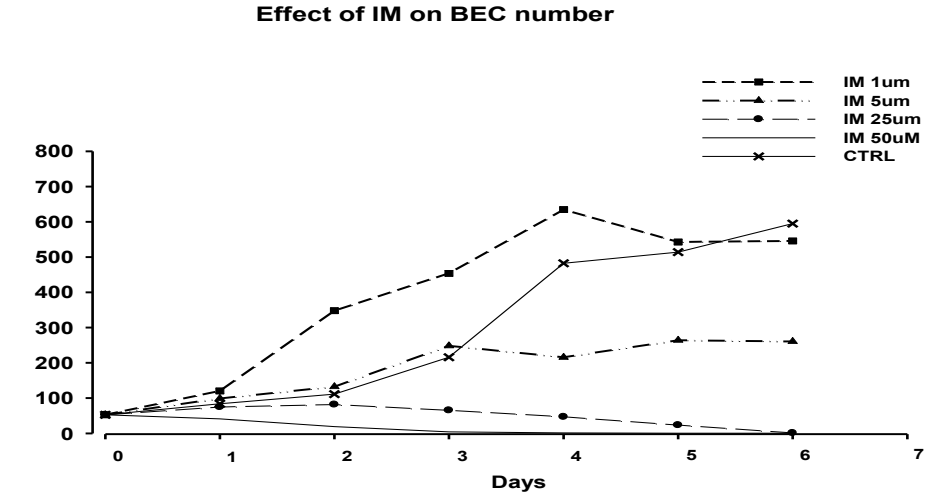

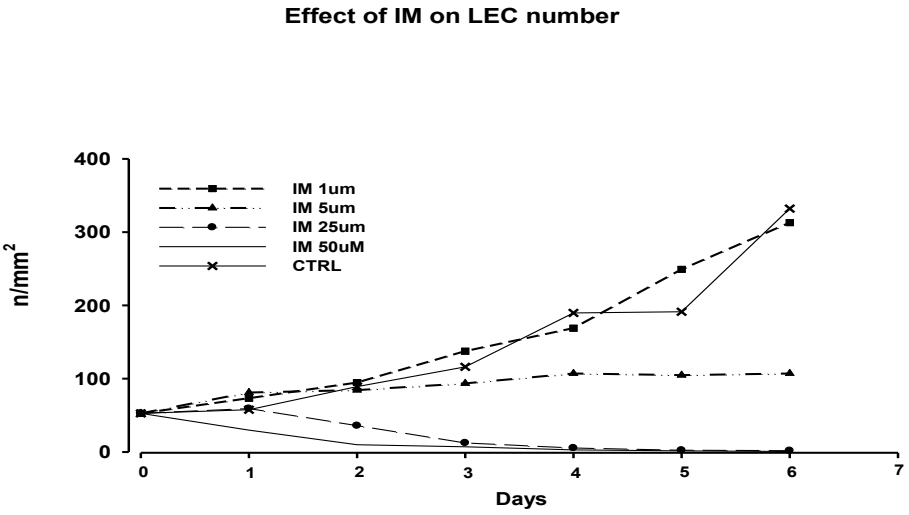

Figure 10. Effects of in vitro treatment with IM on hCPC, hBEC and hLEC.

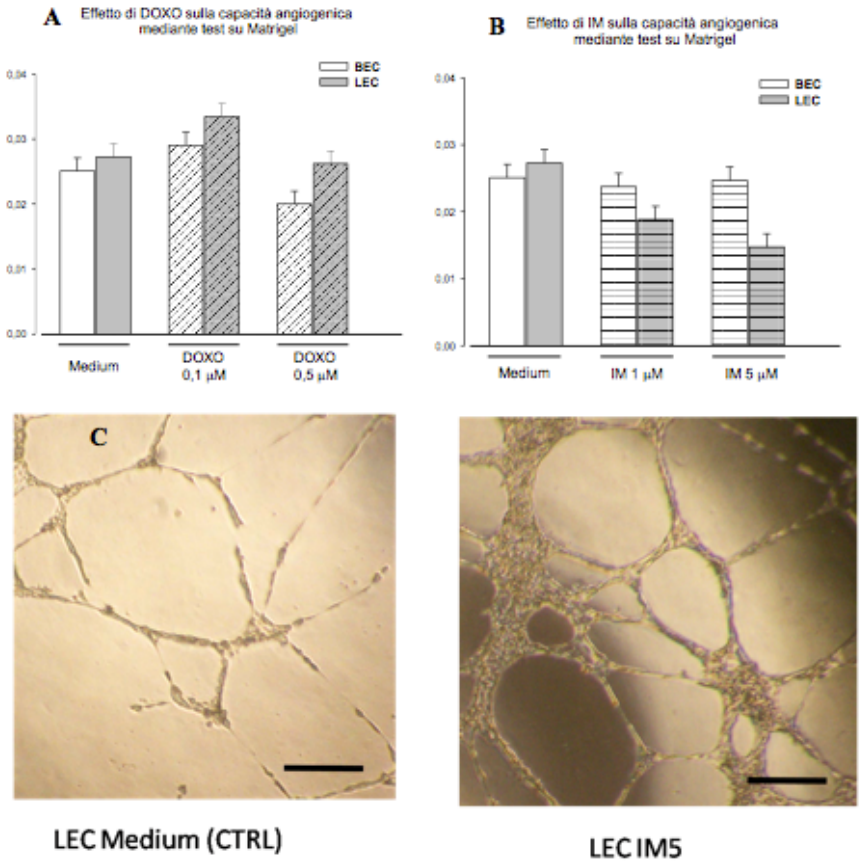

Figura 11: effects of DOXO and IM on angiogenic properties tested with Matrigel assay. Graph A and B show results of matrigel assay on hBEC and hLEC, treated with different concentrations of DOXO(A, 0.1 µM and 0.5 µM) and IM (B, 1 µM e 5 µM).
After treatment with IM5 the ability in forming tube is reduced (fig. C) respect to ctrl (scal bar=250 µM)

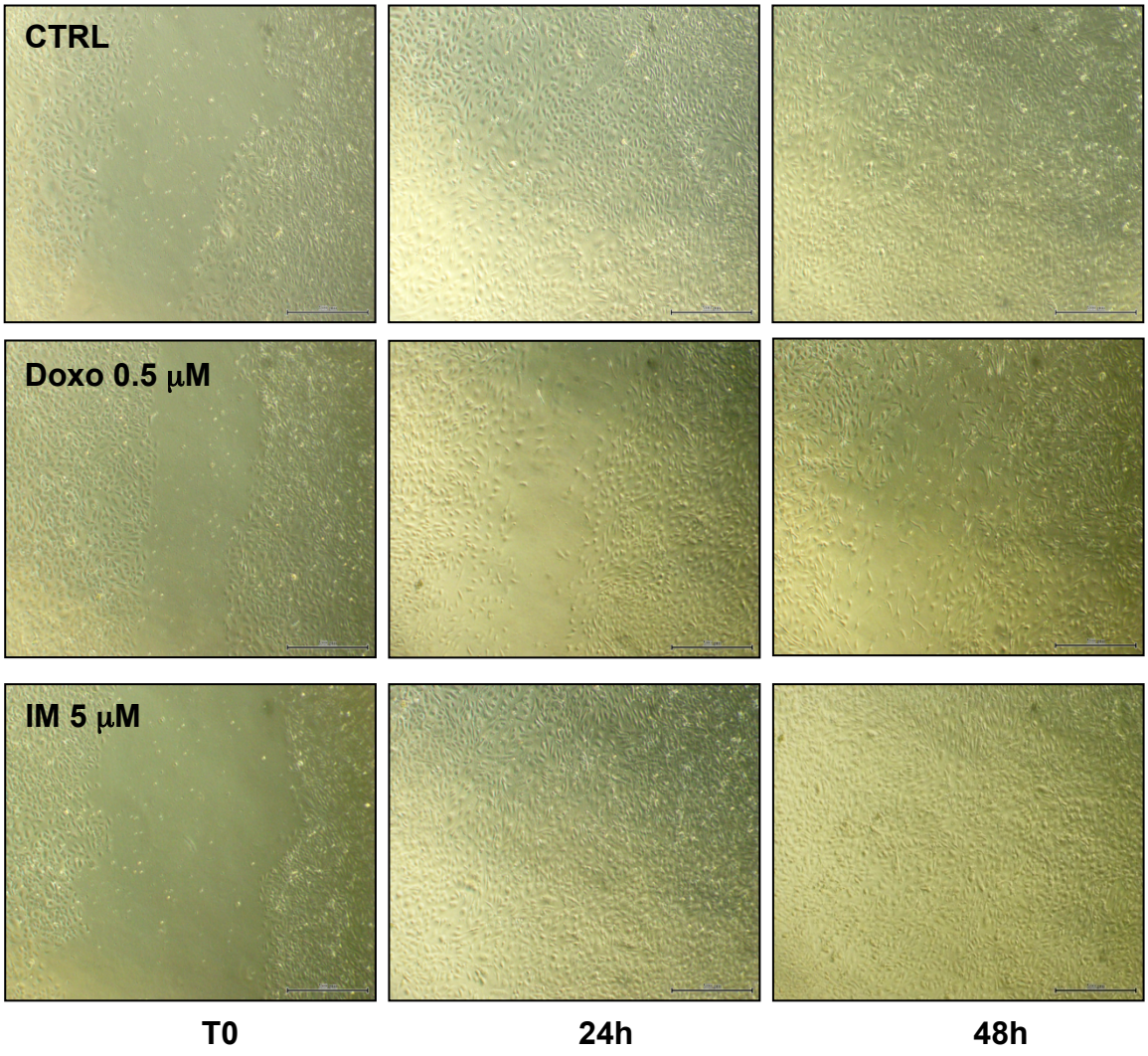

Figure 12: Wound Healing assay of human endothelial cells.
Pictures show the results of wound healing assay observed at different time (0, 24 and 48 hours) with endothelial cells incubated with DOXO 0.5 μM and IM 5 μM.

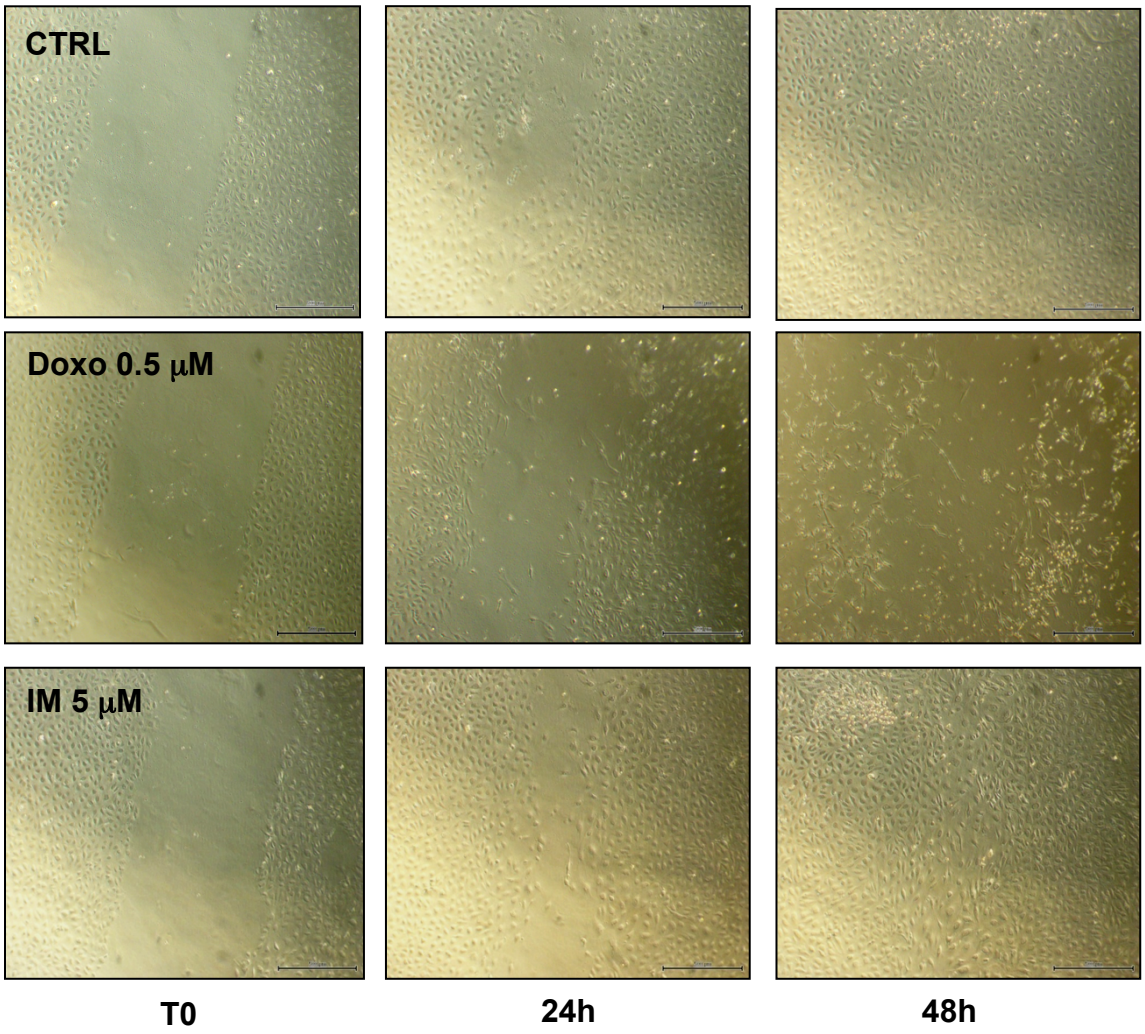

Figure 13: Wound Healing assay of human lymphatic endothelial cells.
Pictures show the results of wound healing assay observed at different time (0, 24 and 48 hours) with lymphatic endothelial cells incubated with DOXO 0.5 μM and IM 5 μM.

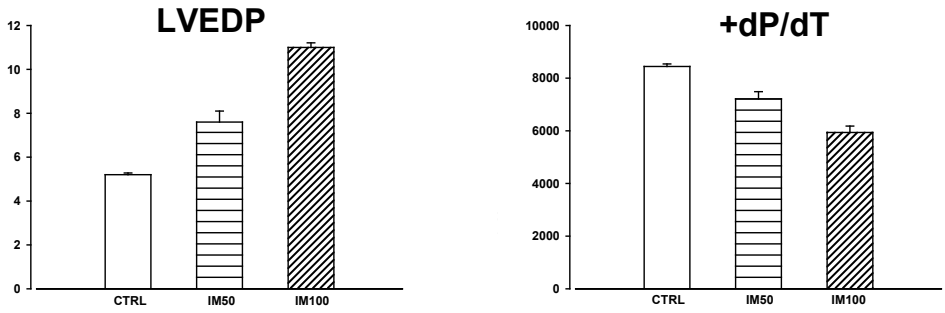

Figure 14. Hemodinamic parameters. Bar graph showing the effect of 50 mg/Kg (IM50) and 100 mg/Kg (IM100) of Imatinib (IM) on Left Ventricular End Diastolic Pressure (LVEDP) and positive dP/dT. A dose dependent impairment in cardiac function was observed. Diastolic dysfunction was present even at low doses of IM. *= p<0.001 vs CTRL;**= p<0,005 vs IM50.

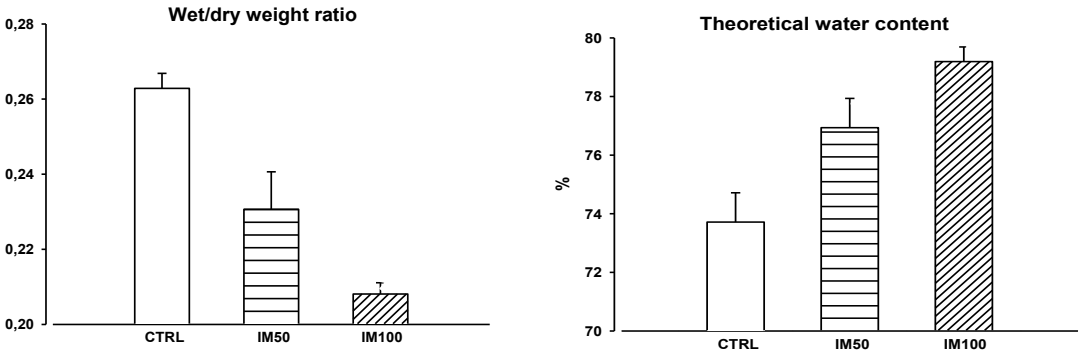

Figure 15. Water content. When the ratio of cardiac wet to dry weight was measured, compared to control values, an increase of theoretical water content in treated hearts was observed, especially with 100 mg/kg doses of IM. *= p<0.001 vs CTRL;**= p<0,005 vs IM50.

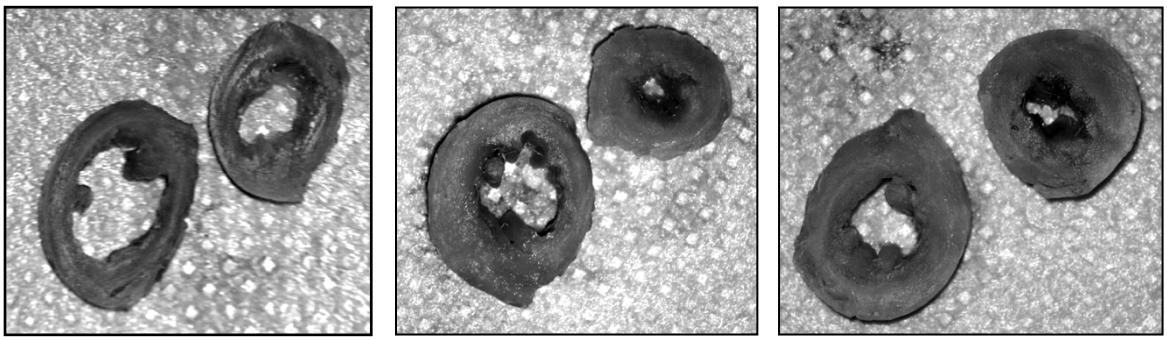

Figure 16. Left ventricular anatomy. Macroscopic view of sections taken at the base and apex of the left ventricle of untreated (CTRL), 100 mg/Kg (IM100), and 200 mg/Kg (IM200) IM treated hearts. Scale bars: 1mm.

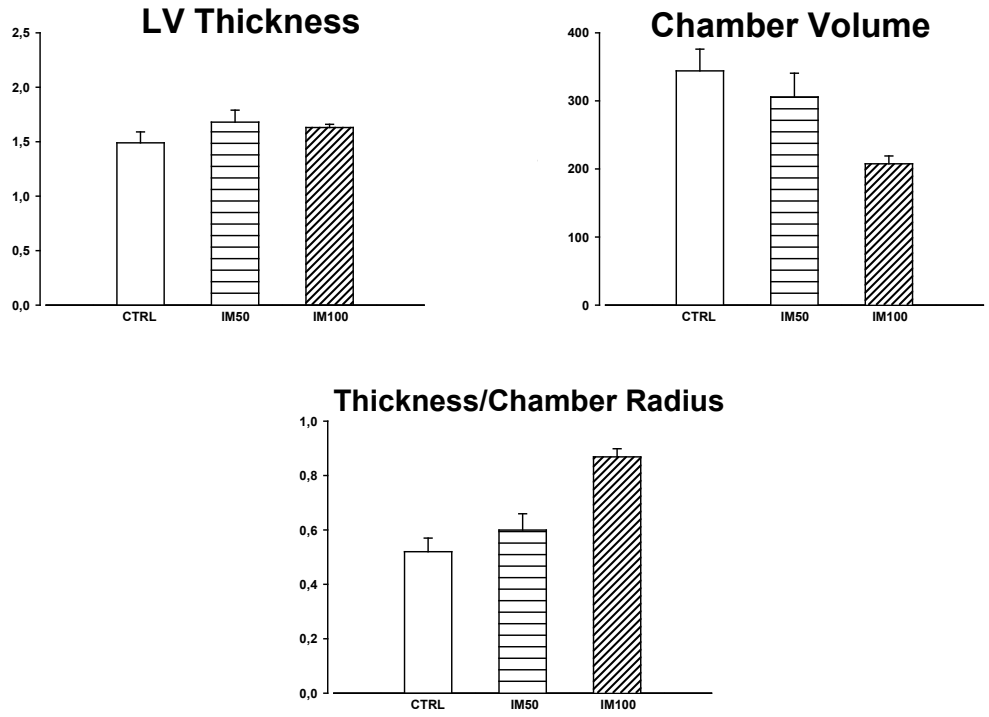

Figure 17. Bar graphs showing the effect of 50 mg/Kg (IM50) and 100 mg/Kg (IM100) of IM on Left Ventricular anatomical parameters. Only high doses of IM resulted in restrictive type of ventricular remodelling. CTRL= untreated rats. *= $p<0.001$ vs CTRL; **= $p<0,005$ vs IM50.

FIBROSIS

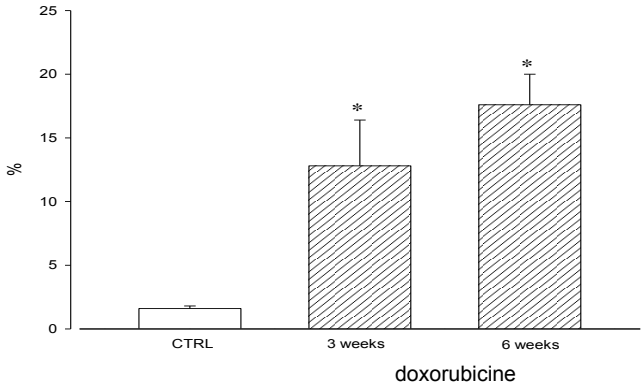

Fig. 18. **Fraction of fibrosis in heart of rats treated with DOXO.** Bar graphs show an increase in fibrotic tissue in a dose and time dependent manner

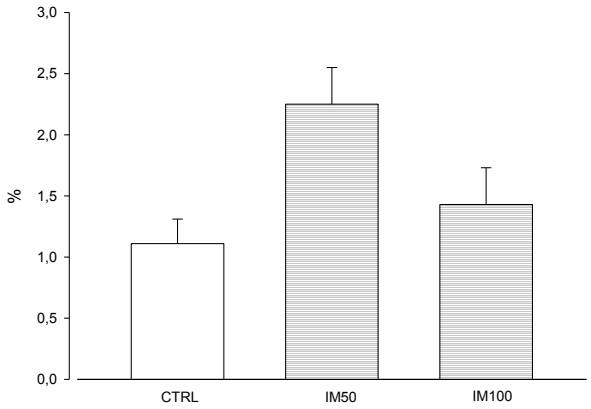

Fig. 19. **Fraction of fibrosis in heart of rats treated with IM50 or IM100.** Bar graphs show an increase in fibrotic tissue in a IM50 and IM100 but not statistically significant.

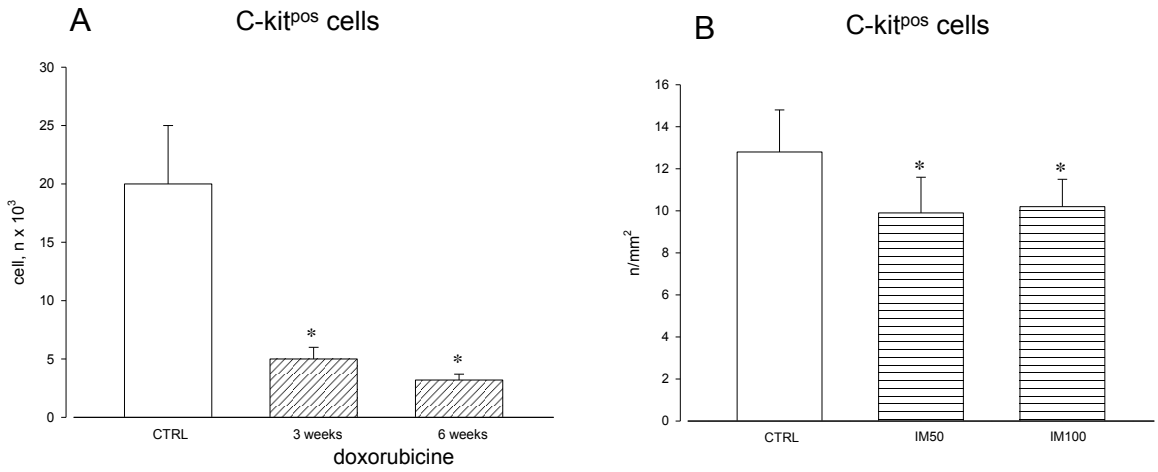

Figure 20. Effect of in vivo treatment with DOXO (A) and IM (B) on number of progenitor cells in rat heart

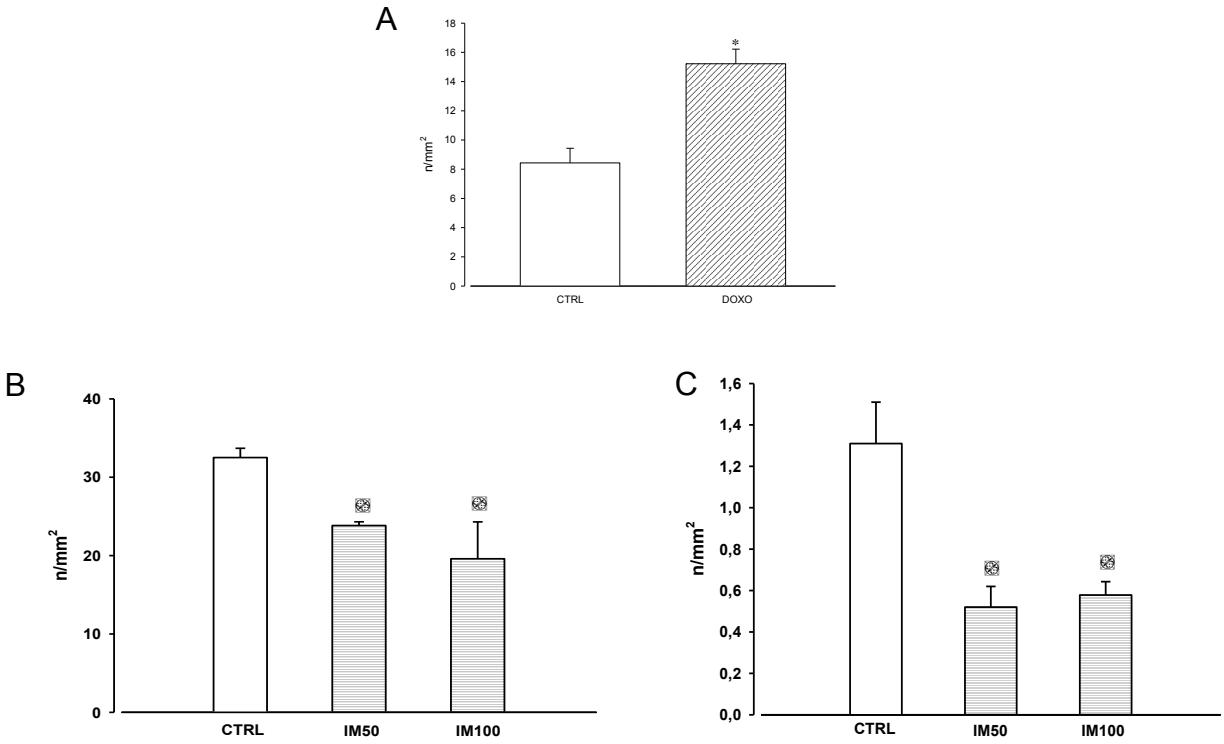

Figure 21. Bar graphs showing the effect of DOXO on lymphatic density (A) and the effect of IM on arteriolar (B) and lymphatic (C) density. *= $p<0.001$ vs CTRL.

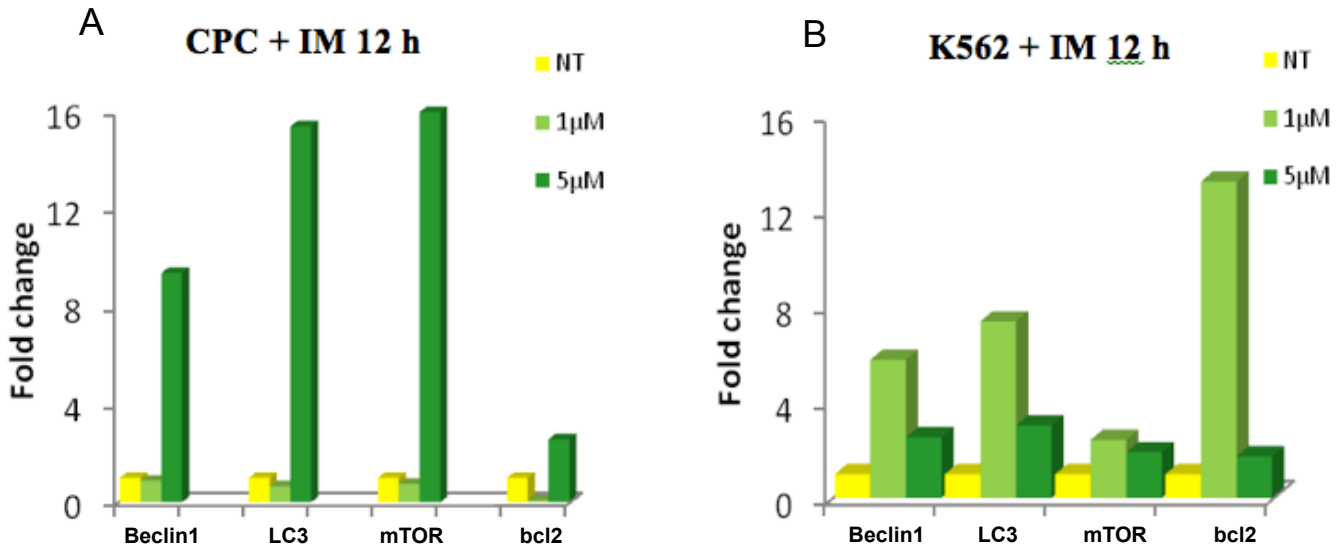

Figure 22. In vitro effects of IM on genetic expression of Beclin1, LC3, mTOR and Bcl2. An increase in all molecule is present after treatment with IM on both hCPC (A) and K562 (B).

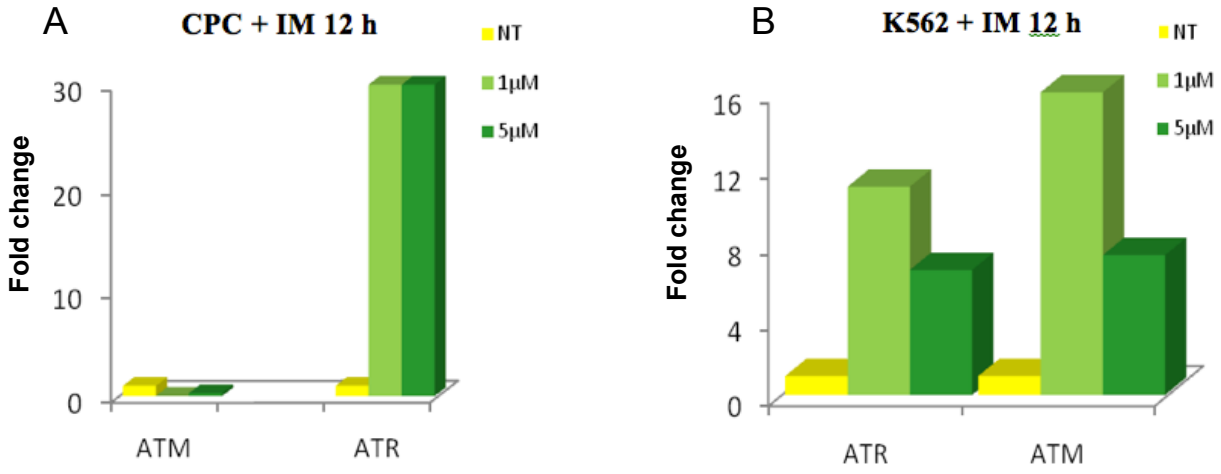

Figure 23. In vitro effect of IM on genetic expression of ATM and ATR. Graph bars show the increase of ATM and ATR after treatment with IM on hCPC (A) and on K562 cell line (B)

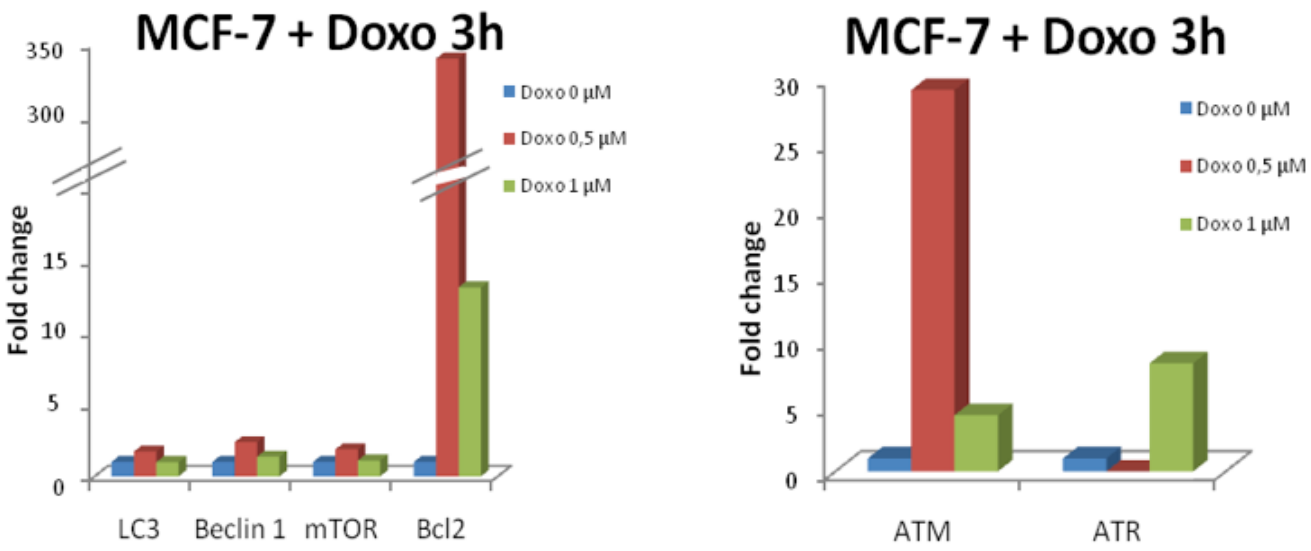

Figure 24. In vitro effect of DOXO on genetic expression of LC3, Beclin1, mTOR, Bcl2 (A) and ATM and ATR (B) in MCF7 after treatment with DOXO. They all result increased after treatment with DOXO.